

Hybrid Machine Learning-Neuromusculoskeletal Modeling for Control of Lower Limb Prosthetics

Andrea Cimolato^{1,2}, Giovanni Milandri¹, Leonardo S. Mattos³, Elena De Momi²,
Matteo Laffranchi¹ and Lorenzo De Micheli¹

Abstract—Objective: Current limitations in Electromyography (EMG)-driven Neuromusculoskeletal (NMS) modeling for control of wearable robotics are the requirement of both Motion Capture for both an indoor system and numerous EMG electrodes. These limitations make the technology unsuitable for amputees with only proximal muscles, who need optimal prosthetic device control during everyday activities. Therefore, we developed a novel Machine Learning (ML)-driven NMS model able to predict lower limb joint torque only from wearable sensors than can be embedded in a prosthetic device. **Methods:** After the NMS model calibration of a single healthy subject (OpenSim® software and Calibrated EMG-Informed Neuromusculoskeletal Modelling CEINMS Toolbox), an additional ML layer (Gaussian Mixture Regressors) was added to the model to replace the MoCap-derived dependent variables with estimations obtained only from wearable sensors. An on-line open-loop Forward Dynamic (FD) simulation of the knee joint is computed and torque trajectories are compared to experimental ones. **Results:** Estimations of the novel ML-driven Musculoskeletal model were comparable with experimental knee joint torque during typical locomotion tasks. Accuracy results were comparable to standard EMG-driven MS models and errors are below the threshold of Normalized Root Mean Square Deviation ≤ 0.30 recognized in literature. **Conclusions:** We developed the first concept of completely wearable and subject-specific EMG-driven NMS model control for lower limb prostheses. The possibility to use this NMS model for FD simulations and the estimation of torque reference control avoids the use of current heuristic and overly complex standard controllers for lower limb prostheses. This research, in fact, represents a key step for the definition of a novel human-machine interface able to create a seamless interconnection between human native control and future wearable robotics.

I. INTRODUCTION

During the last decade, “smart prostheses” were born as a result of innovation in the field of robotics and wearable technologies [1]. Despite their capability to adapt their control interpreting data from embedded sensors, current prostheses are not equipped with actuators, for lighter and more compact designs, and therefore they are not able to provide net-positive power [2]. As a consequence, gait asymmetry and compensatory movements increase biomechanical stresses. In the long term, this contributes to articular pain and often results in chronic disabilities [3], [4]. Nevertheless, in spite

*This work was supported by Istituto Nazionale Assicurazione contro gli Infortuni sul Lavoro (INAIL), within the PPRAI 1/1 project.

¹ Fondazione Istituto Italiano di Tecnologia, Rehab Technologies Lab, Via Morego, 30, 16163, Genova, Italy.

² Neuroengineering and Medical Robotics Laboratory, Dept. Electronics, Information Science and Bioengineering (DEIB), Politecnico di Milano, Building 32.2, Via Giuseppe Colombo, 20133, Milano, Italy

³ Fondazione Istituto Italiano di Tecnologia, Department of Advanced Robotics, Via Morego, 30, 16163, Genova, Italy.

of the great benefits powered prostheses are still far from being practical in a user’s daily life. Indeed, active innovative devices still need to deal with critical cost and usability issues [5]. Based on these premises, the scientific community is particularly interested in the introduction of volitional control, in particular through Electromyography (EMG). In fact, lower limb prosthetics users have no direct control their device: the internal controller through sensors like Inertial Measurements Units (IMUs), encoders and force/torque sensors interprets the condition-state of the device and applies the most appropriate control [6].

However, according to Windrich et al., roughly 80% of the papers they collected, regarding lower limb prosthesis control, published after 2010, are related to EMG-driven control [7]. Despite this effort, such technologies are still not able to provide a reliable Human-Machine Interface (HMI) capable of allowing complete and seamless control of the prosthesis. Therefore, even if the device adopts a control input close to the native biological apparatus, the interface and the control lack the ability to employ it correctly, producing a prosthesis control that is difficult, overly complex and requiring extensive user training. Typically, in order to maximize the controller stability and reliability, bioengineers apply Machine Learning (ML) and pattern recognition approaches to discretize human locomotion in motor tasks and phases. These can be detected and controlled extracting neuro-mechanical features from the embedded sensors [2]. In particular, this approach avoids typical problems related to the EMG signals properties (e.g. non-stationariness and motion artifacts) and the inherent characteristics of the Musculoskeletal (MS) system (high non-linearity, time-varying and redundancy) [8], [9]. In fact, for these reasons, this approach is preferred over the direct control with EMG-signal which is unstable and unreliable due to the signals high variability.

Recently, a deeper understanding of how the Neuromusculoskeletal (NMS) system works has allowed bioengineers to reproduce through simulations the behavior of the biological system. Previous attempts in using MS modeling have been used for the control of prosthetic devices [10], [11]. But, simplifications and approximations were required for the real-time controller, which compromised the prediction of an accurate control reference as stated in [12]. On the other side, complex and dense muscle-tendon unit models require several EMG input channels in order to access their activity level: this particular condition cannot always be guaranteed both for technical reason or because the necessary muscles are missing or not accessible to recording, like in case of am-

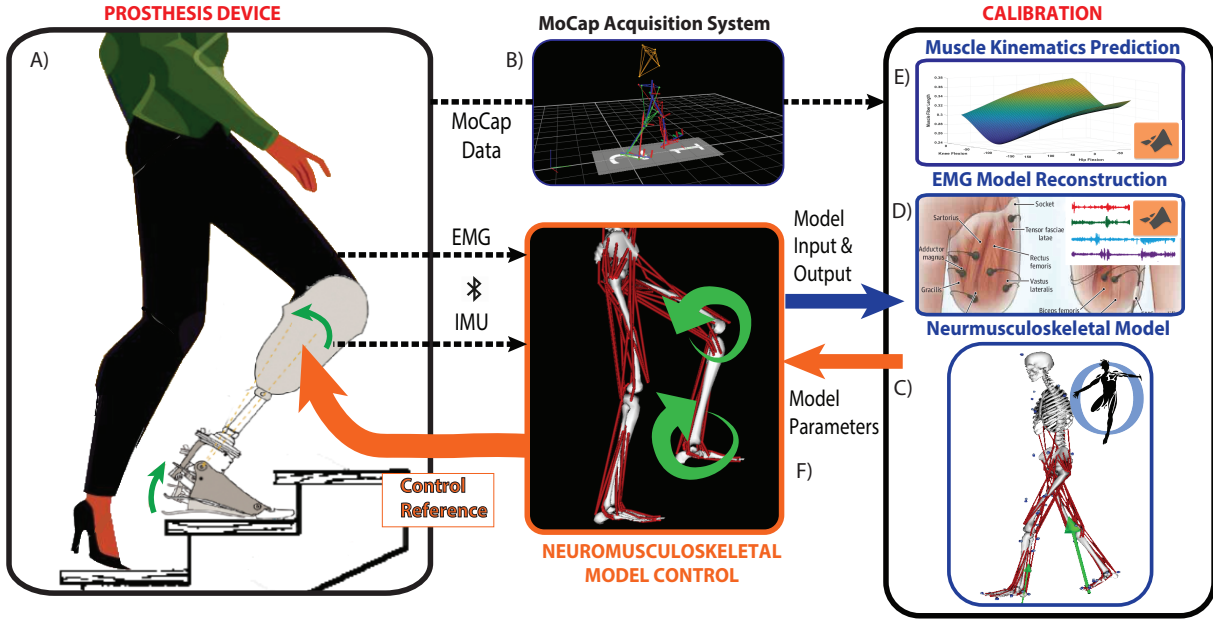


Fig. 1. Schematic representation of the proposed neuromusculoskeletal model control for wearable robotics. A) User wearing the neuroprosthesis, the device is embedded with wireless EMG and IMU sensors; B) Motion Capture (MoCap) acquisition system; C) Musculoskeletal calibration through the motion capture and wearable sensors data. D) Machine learning model training for reconstruction of all the required EMG signals necessary during the EMG-driven forward-dynamics. E) Calibration of the machine learning module for muscle kinematics prediction and muscle moment arms. F) Real-time simulation driven from the wearable sensors as input. Predicted joint torque is used as reference for the control of the neuroprosthesis.

putees. Moreover, subject-specific NMS modeling requires the use of Motion Capture (MoCap) data compromising the portability of the system in a wearable device, such as a lower limb prosthesis.

The objective of this work is therefore to assess the possibility of preserving the high complexity and specificity of human NMS modeling for reliable and real-time estimation, without losing the possibility of integration in a wearable device. Therefore, our work proposes the first EMG-driven FD simulation based on a hybrid approach combining subject-specific NMS modeling and ML for locomotion driven only by sensors that can be embedded in the prosthesis.

II. MATERIALS AND METHODS

The proposed framework requires five steps (Fig. 1): I) Data collection and acquisition protocol (Fig. 1A-B); II) Modeling and calibrating the user NMS model with the acquired MoCap data (Fig. 1C); III) Tuning of a ML algorithm in order to reconstruct all surface EMG (sEMG) required from only a subset of available proximal sensors (Fig. 1D); IV) Calibration of ML algorithm for the estimation real-time muscle kinematics through IMU data (Fig. 1E); V) On-line open-loop simulation of the concatenated models is computed using only the wearable sensors that can be embedded in a future prosthesis prototype (Fig. 1F).

A. Data collection

A single healthy male (age: 28 years, height: 182 cm, mass: 79.5 kg) volunteered for this investigation and gave his written informed consent. The acquired data is divided into calibration and testing trials. Calibration trials comprise 3 static standing trials, 10 on-level walking trials at comfortable self-selected velocity (3.2 km/h), 10 walking trials

at self-chosen higher velocity (5.8 km/h) and 5 trials with 3 squat task repetitions each. Testing trials instead include five different task types: 30 on-level walking trials equally divided at three different increasing speeds (1.5, 3 and 5 km/h; Fig 2B); 10 sit-to-stand and stand-to-sit tasks; 10 stand to walk trials.

In each trial the subject is instrumented with 39 reflective markers (Fig 2A): a modified version of the Plug-In-Gait marker set is used. Motion capture recordings were acquired through MoCap system (VICON®, Oxford, UK); acquisitions at 120 FPS. Split-belt sensorized treadmill (AMTI®, Watertow, MA, United States) provided two platform GRF acquisition each sampled at 1000 Hz. The Ground Reaction Force (GRF) is low-pass zero-phase second-order Butterworth filtered with 12 Hz and 6 Hz cut-off frequencies. All wireless sensors were connected to a COMETA® Wave Plus Wireless 16 digital channels. Two wireless IMU sensors, (COMETA® WaveTrack, MI, Italy) are placed on the front middle of the left thigh and at the tibia (Fig 2A). Quaternions were directly estimated from the IMU sensors and the generated trajectories are low-pass filtered at 6 Hz cut-off frequency with zero-phase second-order Butterworth filters. Due to the preliminary phase of the project, it had not access to amputee subjects, but the EMG setup tried to reflect as close as possible the condition of a left transfemoral amputee (Fig 2A). EMG activity is recorded at 2000 Hz through wireless sensors (COMETA® Mini Wave, MI, Italy) over 9 superficial muscular group in the right tibia and thigh (Rectus Femoris, Vastus Lateralis, Vastus Medialis, Gracilis, Sartorius, Semitendinosus, Biceps Femoris, Lateral and Medial Gastrocnemius) and over the 5 biggest muscles of the upper left leg (Rectus Femoris, Vastus Lateralis, Vastus

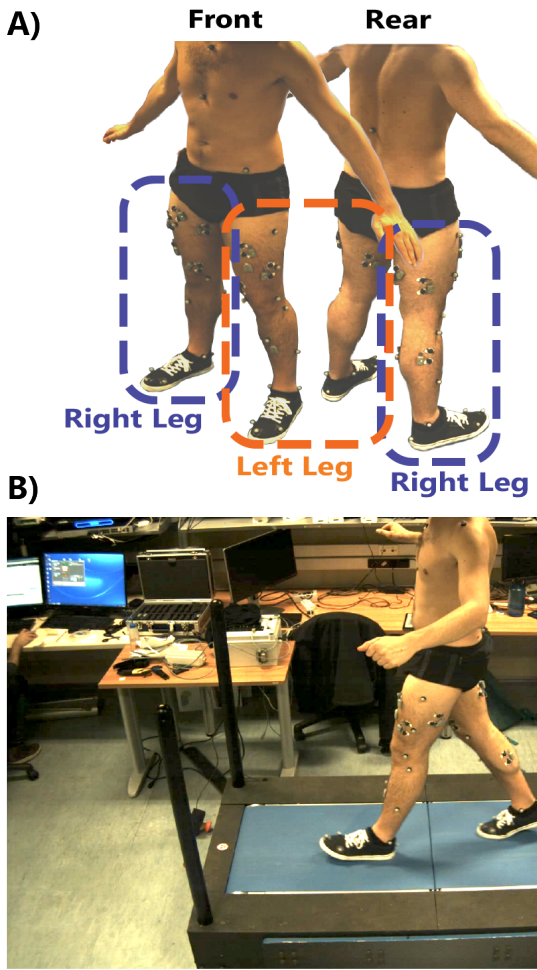


Fig. 2. Subject view during and experimental acquisition. A) User wearing the neuroprosthesis, the device is embedded with wireless EMG and IMU sensors; B) Motion Capture (MoCap) acquisition system;

Medialis, Biceps Femoris). EMG signals are first band-passed filtered between 30 and 300 Hz, full-wave rectified and zero-phase second-order Butterworth filtered at cut-off frequency of 6 Hz. Linear envelopes of each muscle are normalized for their maximum recorded value in the calibration trials set. Synchronization and recording of the signals are performed through NEXUS VICON® Software. Finally, the dataset is converted and exported to OpenSim® and MATLAB compatible files [13].

B. Modeling and calibration of the human NMS model

The MS model used for these analyses is composed of seven rigid bodies: five in each leg (toes, calcaneous, talus, tibia and femur) and two for the main body (hips and torso). The adopted model is described by three-dimensional 37 Degrees of Freedom (DOFs). Main muscle groups are described through 92 Hill-type Muscletendon Units (MTUs) (Fig. 1C). OpenSim® software was used to calibrate the model parameters to match the subject anthropometry using MoCap static standing trials data as described in [14]. Joint kinematics is obtained using the Inverse Kinematics (IK) tool. Angle joints of the calibrated model, similarly to the calibration process, are calculated solving weighted least

squares problem between the virtual and the experimental markers trajectories. Finally employing the Inverse Dynamics (ID) and Residual Reduction Analysis (RRA) algorithms of OpenSim® it is possible to calculate the joints torque combining the GRF measurements and IK results [15]. The joint torques obtained through the concatenation of these methods are referred as the experimental moments and considered as the ground truth values[16].

An alternative pathway of work is instead to define a subject-specific model able to compute the forward-dynamics through the muscle activity and derive the same experimental torques. Calibration of such EMG-driven MS model can be achieved through the use of the software CEINMS [17]. In particular, the model parametrizes three different transfer functions: muscle activation dynamics, MTU kinematics and dynamics. Neural activation is derived from muscle excitations (linear envelope of EMGs) by modelling the muscle's twitch response, which is finally non-linearly related to the muscle activation, the input of the MTU [17]. The parameters regarding muscle activation dynamics vary non-linearly across subjects, due to different anatomic and physiological conditions. Therefore, parameters such muscle twitch activation/deactivation time constants and excitation-to-activation non-linearity factor are calibrated through minimization of the normalized sum of squared differences between predicted and experimental joint moments [15]. MTU kinematics according to [12] is defined as a set of multidimensional splines with the same cardinality of the number of MTUs. Finally, the musculotendon dynamics component is a Hill-type model with initial parameters values inherited from the scaled OpenSim® model. These are refined during the same calibration process of the muscle activation dynamics.

FD NMS model simulations are obtained concatenating the aforementioned blocks in sequence. Recorded sEMG are converted to muscle activations and the joint angle estimated by IK are projected through the spline functions to MTU-specific elongations and moment arms. These values are used as input for the muscle dynamics which in turn generate the MTU linear force that is projected on the moment joint thanks to the estimated moment arms. Such FD is possible only on the right leg, where the full sEMG and MoCap recording are available to compute the 12 MTU models related to the knee. On the left side, exactly as in an amputee stump, is not able to provide all the muscle excitations for the simulation. Therefore the next step is to reconstruct the missing muscles activations from what it was possible to acquire.

C. ML reconstruction algorithm of the sEMG signals

The biggest problem related the introduction of NMS modeling in the control of a prosthetic device remains the impracticability of embedding a high number of EMG electrodes on the prosthetic device. This particular condition can be caused both from the hardware implementation of the device (such as socket adherence, or input channels available in the electronics) and from the anatomy of the amputation, which may have severed essential muscles from the joint. Moreover, since the surgical reattachment and repositioning

of the muscles in the stump is tailored to the type of amputation and patient, muscle position may change a lot and their surface electrical pattern may be very different than in healthy subjects.

For this reason, a ML approach is introduced to cope with these problems. A Gaussian Mixture Regressor (GMR) was used to generate a complete set of sEMG signals starting from the supposed residual subset of available EMGs (Fig. 1D). GMR modeling was chosen both based from previous exploratory attempts with different regression algorithms and literature investigation [18]. The ML algorithm uses the healthy side sEMG (right leg) as template that has to be reconstructed from the reduced set of EMG on the amputated side (left leg). Input data is edited as follows. Walking trial sEMG signals are synchronized according to the walking cycle. This step is not necessary in case of the remaining calibration trials where the tasks are symmetrical with respect the sagittal plane. Real-time acquisition are reproduced processing raw EMG recordings with a 300 ms circular buffer and 50 ms sliding window, filtered accordingly to the aforementioned methods and averaged to a data point.

Randomly chosen 20% of each trials type in the testing set is used as validation set to assess the optimal number of Gaussian Primitives (GP) for the regression. GMRs with incremental number of components are tested on the validation set. Relative differences on the mean Correlation Coefficient lower than 0.01 triggered the end of the optimization process. Phase and magnitude of the reconstructed sEMG with respect to the recorded one are evaluated. Pearson correlation test and Relative Power (RP) signal coefficient

$$RP = \frac{\sqrt{\sum_{i=1}^N X_i^2}}{\sqrt{\sum_{i=1}^N \hat{X}_i^2}} \quad (1)$$

where \hat{X} is the ML estimated variable and X is the experimental one, were calculated.

D. ML algorithm for MTU kinematics estimation through IMU data

Real-time estimation of the IK has been already been investigated through the use of OpenSim® software with TCP/IP direct connection to external MoCap systems through stereo cameras [19]. This setup despite guaranteeing high accuracy on the body movement recording and joint angle tracking, is incompatible with wearable technologies meant to be used during every-day life, limiting the application of this approach to instrumented close rooms. For this reason, this technology is currently shifting toward wearable sensors like IMUs [20]. Such applications can provide analytical solution to the IK problem, but the subject is required to wear at least one sensor per segment in order to estimate the angle between the tracked segments. In particular for lower limb prostheses, due to the presence of bi-articular muscles both in the thigh and in the tibia, the estimation of the adjacent joint angle respect to the prosthetic one is necessary for an accurate estimation of the joint moment to be applied to the prosthesis. Therefore, users of such

wearable technology would need to carry additional IMU sensors on their residual limb/torso to calculate all the necessary muscle kinematics, impacting the comfort and wearability of the system. Moreover since the acceptance of the prosthetic device is usually highly related to the comfort of the system, this will compromise the endorsement of such new technology from [21].

Therefore, the suggested approach proposes the use of only two IMU sensors that can easily be embedded in the two segments of the prosthetic joint, avoiding additional discomfort on the user. In particular for knee torque estimation, the adoption of this configuration (thigh and tibia), does not allow solving the hip and ankle joint trajectories analytically due to the missing information on the relative orientations of the torso and foot with respect to the two mounted IMU sensors. For this reason, similarly to the procedure employed for the EMG reconstruction, a ML approach has been chosen. The MTU kinematics section is therefore replaced by two parallel GMR Models: each one of them, exploits the IMU measured quaternions to estimate, respectively, the muscle fibers elongations and related moment arms, which, were first estimated from MoCap acquisitions. Calibration trial data of the IMU quaternions muscle, fiber lengths and moment arms are extracted with OpenSim® from the calibration trials using the Muscle Analysis tool. The obtained data is segmented with the same window parameters used in the former section, concatenated and fed to the ML training algorithm.

Similarity of the estimated MTU kinematics with respect to the experimental data is quantified with Normalized Root Mean Square Deviation (NRMSD) [16]:

$$NRMSD = \frac{\sqrt{\frac{1}{N} \sum_{i=1}^N (\hat{X}_i - X_i)^2}}{\max(\hat{X}_i, X) - \min(\hat{X}_i, X)} \quad (2)$$

where \hat{X} is the ML estimated variable and X is the experimental one. The number of optimal GPs are assessed on the same validation set used for the EMG reconstruction calibration algorithm. The optimization process aborts once the relative differences in the mean NRMSD is lower than 0.001 m.

E. On-line simulation wearable sensors

After the ML-driven NMS model has been calibrated in all its three components, the system was tested in a open-loop FD simulation, during knee joint movement from the testing trials. Each trials data is processed on-line with the same methodology of calibration. The two IMU quaternion values and the 5 sEMG values of the left leg are segmented with a 300 ms circular buffer and 50 ms sliding window and filtered. Averaged buffer values are then used as input values for the EMG reconstruction and MTU kinematics prediction ML-blocks. The ML-generated muscle activations and fiber elongations are used as input of the Hill-type MTUs of the calibrated NMS model for the computation of their linear forces. Lastly, the generated force is transmitted to the joint as moment through moment arm cross multiplication. Standard EMG-driven MS is instead computed for the

right limb. The complete set of 9 sEMG and the MoCap derived joint angles are segmented as aforementioned and the methodology described in section II.B is applied.

NRMSD values between the experimental torques and the on-line estimations from the ML-driven NMS are used to evaluate the performance of the novel approach. Moreover, we evaluate the obtained results in comparison with respect to standard EMG-driven MS modeling during main locomotive tasks. In this study, as suggested by the literature and previous research groups in EMG-driven MS modeling [16], the target value was $NRMSD \leq 0.3$. Mean computational time of the model between input processing and output generation was calculated. Boundary condition for real-time implementation is represented by the Electromechanical Delay (EMD) in human lower limb (≈ 125 ms [22]).

III. RESULTS

First analyses assessed the goodness of prediction of the two ML algorithms for surface EMG reconstructions and muscle kinematics predictions. Table I shows the correlation coefficients and the relative power coefficient between the 9 recorded sEMG signals from the right leg and the 9 sEMG reconstructed from the left-side using the only 5 EMG signals available. The reconstructed sEMG of the left leg were obtained through GMR with a 4-dimensional GPs. In fact, values in the table shows strong correlation coefficients ($R \geq 0.7$) related to muscles that were directly acquirable in the left thigh. Instead muscles that were not accessible from the electrodes report a lower correlation value ($0.3 \leq R \leq 0.7$). Relative Power coefficients display the same behaviour of the correlation. In particular Vastus, Sartorius and Rectus Femoris muscle groups display highly comparative magnitude ($0.9 \leq R \leq 1.1$) with the ML prediction. Figure 3 displays the recorded sEMG on the right leg with respect to the reconstructed ones from the left leg during the walking cycle. The plotted data reflects the measurements in Table I: similar EMG patterns are generated from the ML algorithm in correlation with the same walking cycle phase.

Instead, on Table II, results are reported regarding the quality of fit between the ML predicted muscle kinematics and the experimental ones for all muscle actuating the knee joint. The predicted muscle kinematics from the IMU wearable sensors with 2-dimensional GMR shows a NRMSD less than 0.3 for all the MTUs with respect to those computed through MoCap. Mono-articular muscles report lower NRMSD values both for the fiber length elongations and moment arms estimation with respect to bi-articular. Only slightly higher deviations from the experimental data can be observed for fiber elongation with respect to moment arms.

The final evaluation of the goodness of the FD knee joint torque trajectories is reported in Table III. Results are a comparison between the literature-validated EMG-driven FD on the right leg (Tab. III, left column) and the novel ML-driven MS FD proposed here on the left leg (Tab. III, right column). Mean NRMSD values are calculated for both the two conditions with respect to the respective experimental knee joint torque estimated through ID, divided in the 5

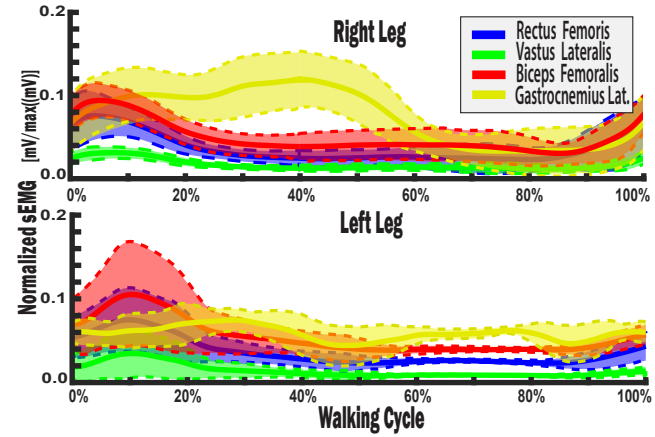


Fig. 3. Results of the EMG reconstruction algorithm for the knee major muscle groups. On the top row recorded normalized envelope of right leg sEMG. On the bottom row reconstructed normalized envelope of left leg sEMG. Bold continue lines represent the mean of the sEMG during test trials normalized on gait cycle

TABLE I

CORRELATION COEFFICIENTS (R) AND RELATIVE POWER (RP)
COEFFICIENTS THE RECONSTRUCTED EMGS AND THE RECORDED ONES.
*: $R \geq 0.7$ (STRONG CORRELATION), *: $0.3 \leq R \leq 0.7$ (MODERATE CORRELATION); **: $0.9 \leq RP \leq 1.1$

Recorded EMG vs. Reconstructed EMG		
Correlation Coefficient	Relative Power Coefficient	
Vastus Lateralis, Intermedius and Medialis	0.82** (SD 0.12)	0.96* (SD 0.20)
Biceps Femoris long and short head	0.71** (SD 0.23)	0.88 (SD 0.15)
Semimebranous/Semitendinosus	0.81** (SD 0.09)	1.11 (SD 0.17)
Sartorius	0.71** (SD 0.22)	1.09* (SD 0.12)
Gracilis	0.45* (SD 0.13)	1.49 (SD 0.93)
Rectus Femoris	0.89** (SD 0.09)	0.99* (SD 0.05)
Gastrocnemius Lateralis and Medialis	0.24 (SD 0.35)	1.27 (SD 0.62)

different types of testing trials. NRMSD obtained for the EMG-driven simulation are coherent with reviewed literature [16]. Deviations from the experimental joint torques are relatively higher for the ML-driven approach but the mean values remain under the suggested limits ($NRMSD \leq 0.3$). In particular, higher deviation coefficients have been obtained for lower velocities walking and for the stand to walk condition. Figure 4 shows the results of the EMG-driven (top row) and the ML-driven (bottom row) on the test walking trials normalized to the walking cycle.

A final test of the ML-driven model was performed to assess the real-time implementation feasibility of the overall model. The model coding and algorithm testing has been

TABLE II

MUSCLE KINEMATICS NRMSD BETWEEN THE PREDICTED MUSCLE KINEMATICS AND THE EXPERIMENTAL ONES. *: NRMSD ≤ 0.3 ; ** NRMSD ≤ 0.1 .

	NRMSD	
	Fiber Elongations [Nm/ ΔNm]	Moment Arms [Nm/ ΔNm]
Vastus Lateralis, Intermedius and Medialis	0.06** (SD 0.07)	0.09** (SD 0.06)
Biceps Femoris long and short head	0.13* (SD 0.15)	0.11* (SD 0.08)
Semimembranosus/ Semitendinosus	0.20* (SD 0.16)	0.11* (SD 0.09)
Sartorius	0.18* (SD 0.14)	0.04** (SD 0.06)
Gracilis	0.19* (SD 0.13)	0.08** (SD 0.09)
Rectus Femoris	0.18* (SD 0.13)	0.09** (SD 0.06)
Gastrocnemius Lateralis and Medialis	0.24* (SD 0.15)	0.14* (SD 0.09)

TABLE III

JOINT KNEE TORQUE NRMSD BETWEEN THE EMG AND ML-DRIVEN PREDICTED KNEE FORWARD DYNAMICS (FD) AND THE EXPERIMENTAL ONE. *: MEAN NRMSD ≤ 0.3 ; ** MEAN NRMSD ≤ 0.15 .

	TRIALS NRMSD	
	EMG-driven FD (Right Leg) [Nm/ ΔNm]	ML-driven FD (Left Leg) [Nm/ ΔNm]
Walking reduced velocity [1.5km/h]	0.10** (SD 0.10)	0.26* (SD 0.35)
Walking medium velocity [3.0km/h]	0.12** (SD 0.10)	0.30* (SD 0.29)
Walking high velocity [5.0km/h]	0.13** (SD 0.15)	0.20* (SD 0.33)
Stand to walk	0.15** (SD 0.31)	0.26* (SD 0.35)
Sit to Stand	0.10** (SD 0.10)	0.21* (SD 0.24)

performed in MATLAB environment with a common laptop (Intel® Core™ CPU 2.21GHz, 16GB RAM). During the on-line testing, the computational time of the ML-driven MS algorithm was calculated for each buffer data. The model simulation is presented with a new input data every 50 ms, this implies that the outer loop of control needs to generate a torque reference point with a frequency of at least 20 Hz. The average open loop estimation of the novel proposed model is in fact below this threshold: the average computational time of the algorithm is 13.64 (SD 16.31) ms for each data point.

IV. DISCUSSION

Despite previous approaches to include EMG-driven control in lower limb prosthetic control, no seamless and effective control has been validated in the literature. One of the

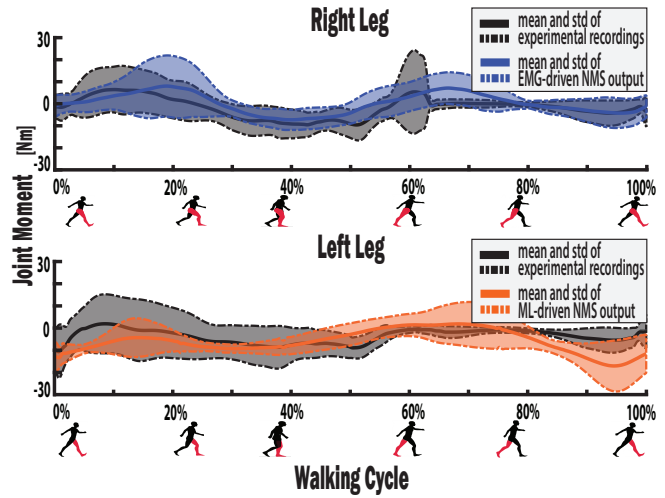


Fig. 4. Mean and standard deviation of the knee joint moment using forward-dynamics during test walking trials. The figure display the mean (bold line) and the standard deviation (dotted line) of the different knee torque trajectories. Data is normalized to the walking cycles and divided into right leg and left leg. The first row estimation of right knee joint moment with standard EMG-driven model (blue) with respect to experimental inverse dynamics calculations (black). Bottom row estimation of left knee joint moment with the developed ML-driven model (orange) respect to experimental inverse dynamics calculations (black).

most promising approaches to avoid issues with EMG-driven control is to employ NMS modeling. In fact, the model itself takes into account the non-linearities of the system, avoiding additional workload on the user. At the state of the art NMS model control suffers particular limitations, like real-time computability and wearability. For this reason, the proposed study aimed in resolve such problems. The contribution of this work can be listed as follows: (i) development of a ML approach for the reconstruction of a whole joint muscles sEMGs from only the biggest most proximal ones; (ii) development of a ML approach for the estimation of muscle kinematics of an entire joint with only 2 IMU sensors; (iii) development of the first subject-specific EMG-driven NMS model for the joint FD estimation for the control of lower limb through only embedded sensors. Preliminary results reported above show that the novel ML-driven NMS model can predict voluntary joint torque generation with an average accuracy of NRMSD ≤ 0.24 (SD 0.11), using only wearable sensors on main locomotion activities. This is achieved through real-time FD simulations of the user-calibrated gait model which describe accurately the NMS system in all its components. Therefore combining this approach with embedded EMG electrodes between the interface with the skin and installed IMU sensors on the prosthesis will allow the user to drive the control reference and move the knee voluntarily.

In particular, we demonstrate that it is possible to reduce the number of electrodes to be embedded in the wearable device. In fact, using a GMR the EMGs necessary to drive the 12 MTUs that actuate the virtual knee were generated from only a sub-set of the required electrodes. The reconstructed EMGs have high correlation coefficients with their recorded counterparts; p-values demonstrate that

the ML-generated EMGs respect the statistical properties of the recorded ones. Moreover, since ML blindly correlates to input data, this will ensure that even with corrupted EMG due to the amputation, reconstruction will be possible. It was demonstrated additionally that through the use of only two IMU wearable sensors estimated quaternions, it was possible to estimate accurately muscle kinematics. Even though wearable technologies have been already used for the estimation of human IK, our approach permits to reduce the distress of the user by limiting the number of acquisition modules located only in the wearable device. Even though missing information on adjacent joints such as hip and ankle, due to the use of only two IMU sensors, compromise the goodness of estimations of bi-articular muscle moment arms and fiber elongations estimations, NRMSD values remain in the accepted boundaries. Finally, we demonstrated the capability of the algorithm to predict in real-time with a comparable degree of accuracy to already validated EMG-driven NMS models in forward joint dynamics. Moreover, results on all the main locomotion tasks, especially in stand-to-walk and sit-to-stand, demonstrate the potential of NMS modes for control of wearable robotics with respect to standard Finite-State Machines (FSM). In fact, such controllers are affected by lower reliability during locomotion transition with respect to cyclical tasks as walking. This is due to the fact that the conditions for FSM transitioning from a control state to the other are difficult to characterize and are usually identified heuristically [2]. In particular, if the tuning of the control is not optimal, the control can generate delays and instabilities whenever the state transition is not recognized [2]. Additionally this generates a limitation that the control cannot act appropriately in case the desired movement has not been included in the control framework. The here proposed control approach, which is EMG-driven, does not require planning and design of the locomotion transitions since the output trajectories depend solely on the virtual MTU activation state and kinematics.

Therefore, the investigated and tested ML-driven NMS model represents an important step for the development of high-level controller for the control of wearable technologies, with particular application for lower limb prostheses. Moreover, the developed control should integrate seamlessly with the biological system control, avoiding difficult learning process or high mental fatigue for the control of the device. Indeed, this will be the focus of future investigations. After evaluation of this proposed approach on multiple subjects, it will be embedded in the control of a powered prosthetic device and compared to standard available controllers. This will create a novel HMI, able to create a seamless interaction between the human native biological system and wearable robotic devices.

REFERENCES

- [1] Torrealba RR, Fernández-López G, Grieco JC. Towards the development of knee prostheses: Review of current researches. *Kybernetes*. 2008;37(9-10):1561–1576.
- [2] Tucker MR, Olivier J, Pagel A, Bleuler H, Bouri M, Lambercy O, et al. Control strategies for active lower extremity prosthetics and orthotics: A review. *Journal of NeuroEngineering and Rehabilitation*. 2015;12(1):1–29.
- [3] Behr J, Friedly J, Molton I, Morgenroth D, Jensen MP, Smith DG. Pain and pain-related interference in adults with lower-limb amputation: Comparison of knee-disarticulation, transtibial, and transfemoral surgical sites. *Journal of rehabilitation research and development*. 2009;46(7):963–972.
- [4] Gailey R, Allen K, Castles J, Kucharik J, Roeder M. Review of secondary physical conditions associated with lower-limb amputation and long-term prosthesis use. *Journal of rehabilitation research and development*. 2008;45(1):15–29.
- [5] Grimmer M, Seyfarth A. Neuro-Robotics. Trends in Augmentation of Human Performance. In: Aramidis P, editor. *Neuro-Robotics: From Brain Machine Interfaces to Rehabilitation Robotics*. vol. 2. Nederland: Springer Netherlands; 2014. p. 105–155.
- [6] Fluit R, Prinsen E, Wang S, Van Der Kooij H. A comparison of control strategies in commercial and research knee prostheses. *IEEE Transactions on Biomedical Engineering*. 2019;67(1):277–290.
- [7] Windrich M, Grimmer M, Christ O, Rinderknecht S, Beckerle P. Active lower limb prosthetics: A systematic review of design issues and solutions. *BioMedical Engineering Online*. 2016;15(S3):5–19.
- [8] Konrad P. *The abc of emg*. vol. 1. 1st ed. Scottsdale, AZ, USA: Noxar INC. USA.; 2005.
- [9] Park H, Durand DM. Motion Control of Musculoskeletal Systems with Redundancy. *Biological cybernetics*. 2009;99(6):503–516.
- [10] Au SK, Bonato P, Herr H. An EMG-position controlled system for an active ankle-foot prosthesis: An initial experimental study. In: 9th International Conference on Rehabilitation Robotics, 2005. ICORR 2005. IEEE; 2005. Chicago, IL, USA: IEEE; 2005. p. 375–379.
- [11] Kannape OA, Herr HM. Split-belt adaptation and gait symmetry in transtibial amputees walking with a hybrid EMG controlled ankle-foot prosthesis. In: 2016 38th Annual International Conference of the IEEE Engineering in Medicine and Biology Society (EMBC). Orlando, FL, USA: IEEE; 2016. p. 5469–5472.
- [12] Sartori M, Reggiani M, Pagello E, Lloyd DG. Modeling the human knee for assistive technologies. *IEEE transactions on bio-medical engineering*. 2012 sep;59(9):2642–2649.
- [13] Mantoan A, Pizzolato C, Sartori M, Sawacha Z, Cobelli C, Reggiani M. MOTO-NMS: A MATLAB toolbox to process motion data for neuromusculoskeletal modeling and simulation. *Source Code for Biology and Medicine*. 2015;10(12):1–14.
- [14] Sartori M, Reggiani M, Farina D, Lloyd DG. EMG-driven forward-dynamic estimation of muscle force and joint moment about multiple degrees of freedom in the human lower extremity. *PloS one*. 2012 jan;7(12):e52618–e52629.
- [15] Sartori M, Lloyd DG, Farina D. Neural data-driven musculoskeletal modeling for personalized neurorehabilitation technologies. *IEEE Transactions on Biomedical Engineering*. 2016;63(5):879–893.
- [16] Sartori M, Gizzi L, Lloyd DG, Farina D. A musculoskeletal model of human locomotion driven by a low dimensional set of impulsive excitation primitives. *Frontiers in computational neuroscience*. 2013 jan;7(79):1–22.
- [17] Pizzolato C, Lloyd DG, Sartori M, Ceseracciu E, Besier TF, Fregly BJ, et al. CEINMS: A toolbox to investigate the influence of different neural control solutions on the prediction of muscle excitation and joint moments during dynamic motor tasks. *Journal of Biomechanics*. 2015;48(14):3929–3936.
- [18] Micheletto S, Tonin L, Antonello M, Bortoletto R, Spolaor F, Pagello E, et al. GMM-based single-joint angle estimation using EMG signals. In: *Advances in Intelligent Systems and Computing*. vol. 302; 2016. p. 1173–1184.
- [19] Durandau G, Farina D, Sartori M. Robust Real-Time Musculoskeletal Modeling Driven by Electromyograms. *IEEE Transactions on Biomedical Engineering*. 2018;64(3):556–564.
- [20] O'Donovan KJ, Kamnik R, O'Keeffe DT, Lyons GM. An inertial and magnetic sensor based technique for joint angle measurement. *Journal of Biomechanics*. 2007;40(12):2604–2611.
- [21] Saradjian A, Thompson AR, Datta D. The experience of men using an upper limb prosthesis following amputation: Positive coping and minimizing feeling different. *Disability and Rehabilitation*. 2008;30(11):871–883.
- [22] Troy Blackburn J, Bell DR, Norcross MF, Hudson JD, Engstrom LA. Comparison of hamstring neuromechanical properties between healthy males and females and the influence of musculotendinous stiffness. *Journal of Electromyography and Kinesiology*. 2009;19(5):e362–e369.